-RESEARCH PAPER-

International Journal of Mining and Geo-Engineering

IJMGE

IJMGE 59-3 (2025) 247-253

DOI: 10.22059/IJMGE.2025.381451.595191

Numerical analysis of the impact of air column length on the rock mass damage zone in air deck blasting operation

Ebrahim Arefmand [a], Hassan Bakhshandeh Amnieh [a, *], Abbas Majdi [a]

[a] *College of Engineering, University of Tehran, Tehran, Iran.*

Article History:

Received: 26 August 2024.

Revised: 03 May 2025.

Accepted: 07 July 2025.

ABSTRACT

In most open pit mines, the first step in the operation cycle of a mining unit is drilling and blasting. One of the most important results of blasting in mines is rock fragmentation. The dimensions of the crushed parts, resulting from the blast, are effective in the costs of loading, haulage, and crushing operations. Many studies have been done in relation to understanding the blasting mechanism and introducing different charging patterns. One of the most practical charging methods that is used today in production blasts in mines is placing an air column along the charging column. This method leads to a change in blast mechanism compared to continuous charging by producing secondary pressures. In this research, the ratio of the optimal length of the air column in the limestone mass has been numerically studied in terms of rock damage. For the analysis and validation of the numerical model of the single blast hole, the field studies of other researchers have been used. In the present simulation, the length of the air column is designed between 0.3 and 0.9 meters. The results represent that by escalating the length of the air column up to 0.7 meters, the pressure applied to the stemming column and fly rock velocity increase with the rate of 1.18 and 1.3, respectively. For longer lengths, this rate increases to 1.58 and 2.39, respectively. It is caused by excessive reduction of the stemming length. The radius analysis of damage in the limestone mass around the blast hole demonstrates that the maximum damage is achieved for the air column with a length of 0.7 meters (air column length ratio was 21.9)..

Keywords: *Air-deck Blasting; Numerical analysis, Rock fragmentation, Damage mechanism.*

1. Introduction

Blast is a rapid physicochemical phenomenon. When the blast occurs, a huge amount of light, heat, and pressure are released [1-2]. Generally, the results of blasting operations include ground and air vibration, fly rock, back break, fragmentation, and movement of the crushed mass. The prediction and control of these factors play an effective role in reducing the total costs of mining operations [3]. One of the most important results of the explosion is rock breakage. Rock breakage can be effective on the results of other activities in the mining cycle (secondary blasting, haulage, and crushing operations). In most conventional mining blasts, less than 20% of the energy produced is devoted to crushing and moving the crushed rock mass, and more than 80% of the energy causes undesirable phenomena [4].

The rock breakage in conventional blasting happens because of two distinct mechanisms. The first mechanism is a compressional stress wave that hits the blasthole wall and expands radially within the rock mass, creating radial cracks around the blasthole. Once the wave arrives at a free surface, it reflects and travels back into the rock medium in the form of a tensile wave causing spalling and creating cracks parallel to the free face.

The second mechanism is the expansion of the products of detonation, applying pressure into the blasthole wall. Although penetration of the gases into the previously formed cracks may contribute to rock fragmentation, the majority of rock damage during the blasting relies on the effect of the stress waves [5]. The conventional blasting method has led to excessive crushing of the rock mass of the hole wall, which is caused by the very high initial pressure of the blast. In this range, a significant part of the energy is lost; therefore, boulders are produced at distances far from the blast hole wall [6-7]. Rock breakage technologies, such as CO2 blasting, instantaneous expansion, slotted cartridge, smoothing blasting, pre-splitting, and chemical demolition agents are efficient ways for blasting damage control in the rock mass [8]. Changing the distribution of explosive inside the blast hole can increase the efficiency of the explosive's energy and improve the results of the blast compared to a continuous charge. Various methods have been proposed for the charging of the blast hole. The decoupling and deck charging methods are the most common blast hole charge methods. The Deck charge method, which is widely used in production blasts, is generally divided into two categories [9].

1- Different explosives are charged in a single hole, and each explosive is charged in one part of the borehole. These different decks of explosives can be charged one above the other without air gaps between them.
2- One explosive is charged in a single hole, but it is separated into several parts by stemming or air.

2. Fracture pattern induced by single-hole blasting

A single-hole detonation experiment in Plexiglas by Johansson and Persson clearly showed that (1) the original borehole expanded, (2) a fractured zone appeared surrounding the borehole, and (3) outside the fractured zone there was a shock or stress wave. Since the 1970s, a great number of blast experiments have proven these observations.

Figure 1 shows the blasting results from a PMMA plate. The plate had a size of 30 cm × 30 cm × 1 cm. At the center of the plate there was a hole

* Corresponding author: *E-mail address:* hbakhshandeh@ut.ac.ir (H. Bakhshandeh Amnieh).

in which a detonator with a diameter of 7 mm equal to the diameter of the hole was inserted as the explosive charge. In other words, this is similar to a full-charge situation. Figure 1 indicates that the fracture pattern consists of the following zones:

1. Expansion zone (empty hole) whose diameter is d_ex=1.3 cm=1.8 ×d, where d is the diameter of the borehole.
2. 2. Over-crushed zone whose diameter is $d_{o-cr} = 2.55\ cm = 3.6 \times d$

3. Crushed zone whose diameter is $d_{cr} = 5.45\ cm = 7.8 \times d$

4. Cracking zone. There were seven long radial cracks which propagated through the plate and made it disintegrate completely [9-10].

In brief, there are two crushed zones: one large crushed zone and one small over-crushed zone. In both crushed zones, the material is fragmented by radial cracks and longitudinal crushing. Figure 1(B) clearly shows that the radial cracks transit the crushed zones, probably starting from the hole [9-10].

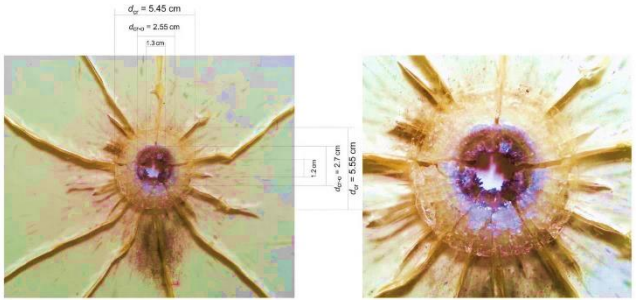

(a) (b)

Figure 1: Crushed zone and cracks in a PMMA plate by full charge. The sizes of the PMMA plate were 30 cm long, 30 cm wide, and 1 cm thick (the pictures show only part of the plate). The diameter of the blast hole was 7 mm. The charge was an electric detonator with a diameter of 7 mm. The two pictures show the same blast in the same plate. (A) Fracture pattern with sizes; and (B) part of the fracture system [9].

The purpose of this research is to review the previous studies to understand the mechanism of air deck blasting, the results of this blasting method, and how to calculate the length of the air deck. Then, the optimal air deck length ratio for the limestone mass is studied using numerical analysis and field results of Singh et al. (2012).

3. Air deck blasting

The air deck blasting method brought significant changes in blasting engineering and provided a new definition for rock breaking by blasting. The air deck blasting method was first proposed by Sanders in 1891 in Germany [11]. This method leads to an increase in the energy efficiency of the explosive material based on energy redistribution. In general, the use of the air deck along the hole has been introduced as a method to improve fragmentation and reduce the consumption of explosives, reduce drilling, and reduce the destructive results of blast [12-13]. An air deck can be in three different positions of the hole (top, center, and bottom) and even in long holes, several air decks can be used along it. Numerical, analytical, and laboratory studies of previous researchers explained air deck blasting mechanism in such a way that in this method the initial hole pressure decreases due to the movement of blasting products into the air column. The shock waves inside the blast hole interact with either the stemming column or the end of it. Repeated interactions lead to producing strengthened secondary shock front and allowing shock waves to act on the surrounding rock mass for a longer time. The reduction in initial shock wave pressure combined with the prolonged loading duration of secondary waves in the air decking method leads to a decrease in the powder zone and expansion of the fracture zone within the rock mass compared to the fully charged blasting method. This phenomenon has been described in detail by Arefmand et al. [14]. This increases the energy efficiency of the explosive and improves the blasting results. The details of the air deck blast mechanism are described in [6-7-14-15-16-17-18-19]. Several researches have been conducted to investigate the effect of air deck on the performance of blasting, which helps to implement this method as properly as possible. Mead et al. (1993) reported the use of air deck blasting in copper, iron and, coal mines. The air deck factor (ADF) varied between 0.35 and 0.45. In these blasts, the consumption of explosives was reduced by 15 to 35%, without having a negative influence on rock fragmentation [20]. Sahran et al. (2017) recorded the duration of stemming maintenance equal to 14.7 milliseconds in conventional blasting and 76 milliseconds in air deck blasting. Furthermore, the average initial velocity of stemming ejection was calculated 250 and 380 m/s for air deck and conventional blasting, respectively [21]. Chen et al. (2017) studied explosive consumption in air deck blasting (air column at the bottom of the hole) compared to conventional blasting. They found that the specific charge is reduced by 11.5 and 13.5% for 80 and 100 cm air deck, respectively [22]. Balakrishnan and Pradhan (2018) showed that the use of hollow plastic tubes (to create an air column) inside the blast hole leads to a noticeable savings of explosives (about 11%) and improved rock mass fragmentation. Moreover, this method reduces CO2 gas emission [23]. Jang et al. (2018) showed by conducting field blasts that the presence of an air deck at the bottom of the blast hole ends up in a significant reduction of powder zone and an increase the uniformity of rock mass fragmentation [24]. Bakhshandeh et al. (2019-2020) showed that air deck blasting leads to improvement of fragmentation (24-35%), reduction of back break (17-55%) and improvement of technical and economic parameters (specific charge (28%), specific drilling and blast hole productivity (9%) compared to conventional blasts [25-26]. Cheng et al. (2022) investigated the effect of position, length, and number of air decks on ground vibration using field and numerical studies. The field results showed that increasing the air deck length ratio can reduce the ground vibration in nearby regions. In addition, the existence of an air deck at the top of the blast hole can reduce the ground vibration in the nearby regions more than the center and bottom positions of the blast hole [27]. The numerical analysis results of Gao et al. (2023) showed that the presence of the air deck at the end of the blast hole can reduce the damage caused to the tunnel surface compared to conventional blasting. This performance is due to the decrease in the initial pressure applied to the tunnel surface. They were able to reduce the time of tunnel face scaling by 15 minutes by air deck blasting [8].

4. Air deck length ratio

The most important parameter to achieve the goals of air deck blasting is the correct calculation of the air deck length. To determine air deck length, the Air Deck Factor (ADF) was used, which is equal to:

$$ADF = \frac{ADL}{OCL} \quad (1)$$

In the above equation, ADL is Air Deck Length and OCL is Original Charge Length. OCL is equal to the sum of charge length (Le) and air deck length (La). Therefore, the above equation can be rewritten as follows [15]:

$$ADF = \frac{L_a}{L_e + L_a} \quad (2)$$

Mel'Nikov and Marchenko (1979) proposed a guideline for determining air deck length according to the following equations based on the experimental results of field blasts [15]:

$$ADL = K_1 \times OCL \quad (K_1 = 0.15 - 0.35) \quad (3)$$

$$ADL = K_2 \times d \quad (K_2 = 8 - 12) \quad (4)$$

In the above equations, air deck length, Original Charge Length, and charge diameter (d) are in meters. K1 and K2 are rock factors. Coefficients K1 and K2 decrease with increasing rock mass strength [15]. Zhang (1996) investigated the effect of changing air deck length at the bottom of the blasthole on rock fragmentation in open pit mines. The

optimal air deck length ratio was determined to be between 20% and 25%. In this study, the air deck length ratio is defined as La/Le [28]. Jhanwar and Jethwa (2000), Jhanwar et al. (2000) and Jhanwar (2011) based on direct observations and field data analysis, presented the feasibility of air deck blasting and guidelines for determining the air deck factor (ADF) for different rock masses in open pit mines (Tables 1 and 2) [29-30-31].

Table 1. Feasibility of air deck blasting for various rock masses.

No.	Type of rock mass	Feasibility
1.	Very low to low strength Sedimentary rock	Excellent
2.	Very low to low strength Sparsely jointed rock	Very good
3.	Medium strength Sedimentary rock (Blocky type), closely jointed rock	Good

Table 2. Air deck length for different rock masses

No.	RMR	ADF
1.	20-35	0.3-0.4
2.	35-45	0.2-0.3
3.	45-65	0.1-0.2

According to the mechanism of air deck blasting and using wave equations, Lu and Hustrulid (2003) provided the following ranges for air deck factor (ADF) [18]:

$$0.135 \leq ADF \leq 0.398 \quad (5)$$

$$0.164 \leq ADF \leq 0.374 \quad (6)$$

Saqib et al. (2015) found that by conducting blasting on a laboratory scale on concrete blocks, the best position of the air deck is the center of the hole with the air deck length ratio of 0.2 to obtain optimal fragmentation [32].

5. Blasting single-blasthole in limestone rock mass

Singh et al. (2012) used a single-blasthole in a limestone rock mass to investigate the propagation of damage due to air deck blasting. The diameter and depth of the hole were considered equal to 0.115 and 4 meters, respectively. The charging method is shown in Figure 2 (A). In this test, ANFO explosive was used as the main charge and drilling powder was used as stemming. After blasting a single-blasthole using an air deck, the damage radius was measured as 2 meters (damage area 4 meters) (Figure 2 (B)) [33]. Due to the operational limitations and the cost of field blasting, in this research, Singh's field results have been used to calibrate the numerical model.

6. Numerical analysis of rock mass damage caused by air deck blasting

Numerical modelling is one of the research methods that saves time and reduces costs; therefore, it is one of the most widely used methods in blasting engineering [8]. Therefore, in this research, numerical modelling has been used to determine the optimal air deck length ratio for limestone rock mass. Model geometry construction, meshing, solution method selection, and material model and material state assignment are as follows.

6.1. Model geometry, meshing, and solution method selection

The first step of numerical modelling is geometry construction and model meshing. According to Figure 3, the dimensions of the model were 5*6*10 cubic meters. In this simulation, the boundary conditions were defined in such a way that the upper boundary is a free surface, the front boundary is a symmetry surface, and the rest of the boundaries were non-reflective. According to Figure 4, based on the convergence test, the size of elements in the perpendicular direction to the blast hole wall was from 15 mm (near the blast hole) to 100 mm (near the model boundary) and 70 mm along the blast hole was designed. It should be noted that the blast hole geometry was designed according to the Singh's experiment (Figure 2). In order to reduce the calculation time, using the symmetry hypothesis, only half of the model has been built [34].

A: Charging B: Damage around blast

Figure 2. Demonstrating the charging method and damage around the blast hole caused by the field air deck blasting [33].

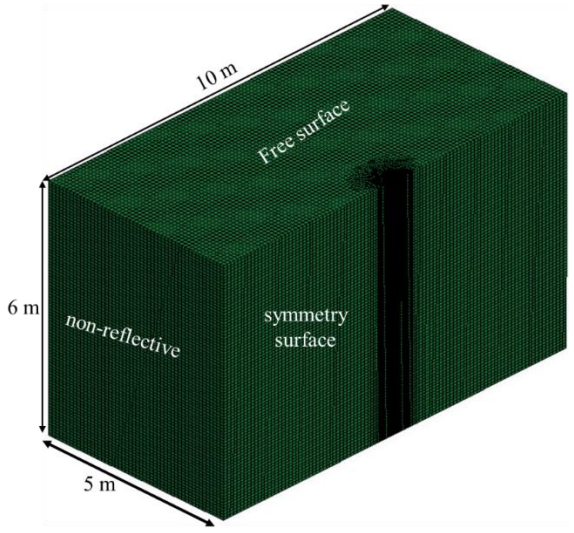

Figure 3. Model geometry, meshing, and boundary conditions of a single blast hole in the limestone rock mass.

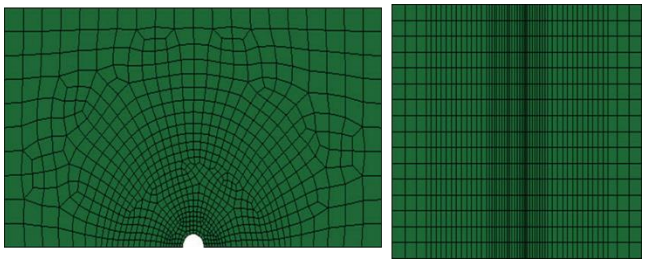

Figure 4. Meshing in two directions. A: perpendicular to blast hole wall, and B: Along blast hole

In this simulation, the Arbitrary Lagrangian Eulerian (ALE) method, which allows the mesh to move independently of the material flow, was used to model rock mass blast [5-19].

7. Rock mass model

RHT rock material model is an advanced plasticity model for analyzing the behavior of brittle structures under impulsive and dynamic loads. This material model was developed by Riedel et al.

(1999) [5]. Therefore, in this simulation RHT was defined as the limestone material model. The characteristics of the rock material model are summarized in Table 3.

Table 3. The parameters of limestone material model [33].

E (GPa)	D (Ton/m³)	UCS (MPa)	Ts (MPa)
30	2.5	50	7

RHT uses a normalized form of effective plastic strain as a damage function, which is a scalar parameter, increasing monotonically whenever the state of the stress in the material is at the yield point. The damage is defined as:

$$D = \sum \frac{\Delta\varepsilon^p}{\varepsilon^f} \quad (7)$$

where $\Delta\varepsilon^p$ is considered as the accumulated plastic strain and ε^f is the failure strain. D is a value between 0 and 1, where D = 0 is a state that the material is undisturbed and D = 1 is a state in which the material is unable to carry tensile loads [5].

8. Explosive model

The MAT-HIGH-EXPLOSIVE-BURN material model is used to model the explosive material, and the JWL equation of state is used to calculate the expansion of the blast products [5-19-27-33]. The equation of state of JWL is defined as equation 8:

$$P = A\left[1 - \frac{\omega}{R_1 V}\right]e^{-R_1 V} + B\left[1 - \frac{\omega}{R_2 V}\right]e^{-R_2 V} + \frac{\omega E}{V} \quad (8)$$

where P is the blast pressure, A, B, R1, R2 and ω are constant coefficients of the equation (it varies for different explosives). E and V are the detonation energy per unit volume and the relative volume, respectively. The input values for the JWL equation of state and related properties of ANFO explosives are given in Table 4.

Table 4. The JWL equation of state parameters of ANFO [33].

A (GPa)	7
B(GPa)	3
R_1	5.5
R_2	0.9
ω	0.24
E (j/kg*10⁶)	3
Density (Kg/m³)	900
VOD (m/s)	2500
Blast pressure (GPa)	3.5

9. Air model

The air is modeled by the material type of MAT_NULL with the specified linear polynomial. This EOS defines the relationship between pressure, density, and internal energy, which is described in [27].

$$P_a = C_0 + C_1\mu + C_2\mu^2 + C_3\mu^3 + (C_4 + C_5\mu + C_6\mu^2)E_r \quad (9)$$

where Pa is the air pressure and C0, C1, C2, C3, C4, C5, and C6 are user-defined constants, Er is the internal energy, and μ is the compression parameter, expressed as μ = 1/V − 1, where V is the relative volume. The parameters referred to by Cheng et al. (2022) are listed in Table 5 [27].

10. Validation of numerical modelling

After finishing the process of modelling and assigning properties related to each material, the blasting of the single blast hole was done completely and the damage radius around the hole was measured. According to Figure 5, the damage radius from the center of blast the hole was estimated at 1.84 meters (charging method according to Figure 2 (A)). The damage zone measurement has been done on the top surface (head of the borehole). In Singh et al.'s field blast, the damage radius around the blasthole was measured 2 meters. It should be noted that all parameters of charging and rock mass in field blasting and numerical modelling are the same. The simulation accuracy against Singh's field [33] measurements is 92%. Therefore, the results show that the constructed numerical model has an acceptable accuracy for investigating the effect of air column length on damage radius around the blast hole. Figure 6 shows the spread of damage around the hole resulting from Singh's blast hole simulation. In fact, Figure 6 shows the damage on the ground surface from the top view, which is the result of the 3D modelling of the problem, according to the explanation section of the numerical model of the problem.

Table 6 illustrates the comparison of blasting pattern and damage zone radius caused by Singh's field blast and numerical simulation done in this paper.

Table 5. The parameters of the air and EOS [27].

Air Density (Kg/m³)	V	E_r (j/cm³)	C_0	C_1	C_2	C_3	C_4	C_5	C_6
1.255	1	0.25	0	0	0	0	0.4	0.4	0

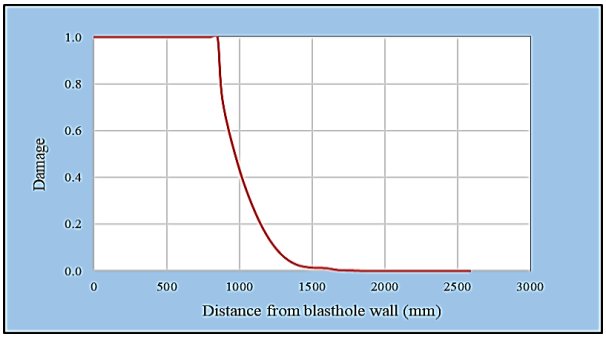

Figure 5. The amount of damage according to distance from blast hole wall on surface.

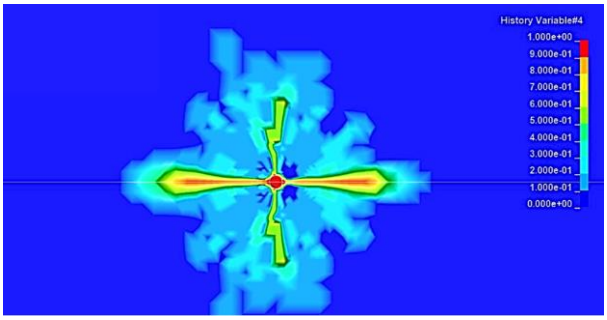

Figure 6. The damage model due to simulation air deck blasting (air deck length = 0.5 m)

It should be noted that the damage zone around the blasthole is determined based on the criterion of D > 0 (According to equation 7). In fact, the elements whose damage value is greater than zero are located in the damage zone.

11. Air deck length ratio effect on damage area

After validating the initial numerical model, the effect of air deck length ratio on the damage around blasthole was studied using numerical analysis. For this purpose, according to Figure 7, eight different charging patterns, modelling, and their results were compared. As can be obs erved, in all charging patterns, the explosive length is constant and equal to 2.5 meters. In charging patterns, the air deck and stemming column length have been changed. This has been done in

Table 6. The comparison of blasting pattern and Damage zone radius caused by Singh's field blast and numerical simulation done in this paper.

Type of blast	Numerical simulation of blast	Field blast (Singh et al)
Blasthole diameter (mm)	115	115
Length of explosive (m)	2.5	2.5
Length of air (m)	0.5	0.5
Length of stemming (m)	1	1
Damage zone radius (m)	1.84	2

order to determine the optimal ratio of air deck length for obtaining maximum efficiency of explosive energy in the limestone rock mass. In the built numerical models, the air deck length ratio was designed between 10.7% and 26.5%.

After the completion of the blasting process caused by charging patterns, the amount of damage was estimated in terms of the distance from the blast hole wall for each blast. The changes in the radial damage rate around the blasthole are shown in Figure 8. The results showed that as the length of the air deck increased from 0.3 m to 0.7 m, the radius of complete damage of elements increased incrementally, and after the length of 0.7 m, the radius of complete the damage of the elements around the blast hole decreased. For the air deck with a 0.9 m length, the damage radius was completely reduced at once.

Figure 9 shows the maximum distance from the blast hole wall where complete damage has occurred for different charging patterns. As can be seen, for the air deck with a length of 0.7 m, the complete damage of the elements has occurred up to a distance of 1 m from the hole wall, which is more than that of the rest of the charging patterns.

The air deck blasting results show that in the limestone rock mass, the optimal air deck ratio is equal to 21.9 in the damage of the rock mass. For blasting patterns with an air deck length greater than 0.7 m, the surface damage decreases abruptly, which can be caused by an excessive reduction in stemming length and the instantaneous throwing of stemming materials. For more transparency, the reasons for changes in damage radius in different charging patterns were investigated in the applied pressure and the movement velocity of the highest element in stemming.

12. Pressure

In order to investigate the causes of damage radius changes in different charging patterns, the blast pressure applied to the highest point of the stemming column was recorded. According to Figure 10, with an increase in the air deck length, the maximum pressure applied to the highest point increased. Table 8 shows the ratio of pressure changes of each charging pattern compared to the previous pattern. From the length of 0.3 to 0.7 m, with the rising air deck length, the applied pressure increased by an average of 1.18 times, while for the length greater than 0.7 m. This increase became equal to 1.58, which indicated that the length of the stemming column was too short.

13. Velocity

Figure 11 shows the trend of changes in the maximum velocity of stemming column for different charging patterns. With increasing air deck length, the maximum velocity of the throwing stemming column increases by an average of 1.3 times (up to a length of 0.7 m), and for lengths greater than 0.7 m, the average ratio of velocity increase equals to 2.39 (Table 9). This is because of the high pressure applied to the top of the stemming column due to excessive reduction of stemming column length.

14. Conclusions

In this research, changes in the air deck length ratio have been studied using numerical modelling and field test results of Singh et al. (2012) in terms of limestone mass damage. This study was done in order to

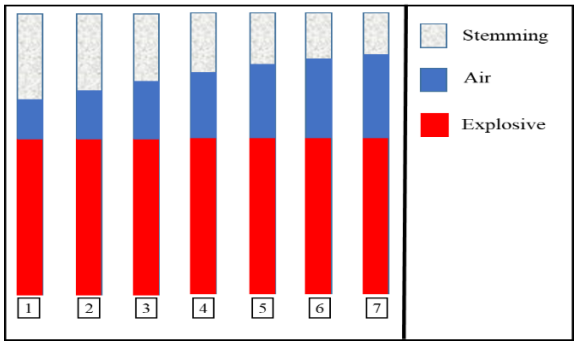

Figure 7. Different charging patterns inside the blasthole in the limestone rock mass

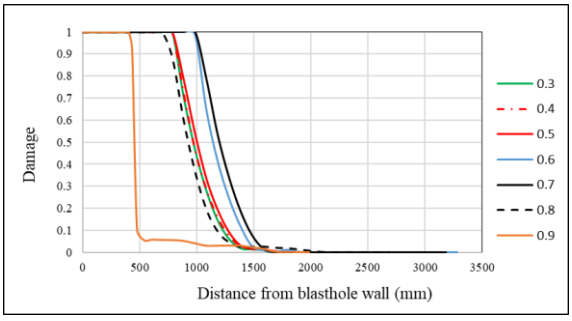

Figure 8. The comparison of damage radius around the blast hole due to changing length of the air deck.

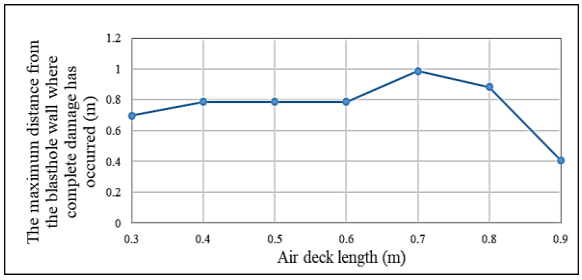

Figure 9. Maximum distance from the blast hole wall where complete damage has occurred for different air deck lengths.

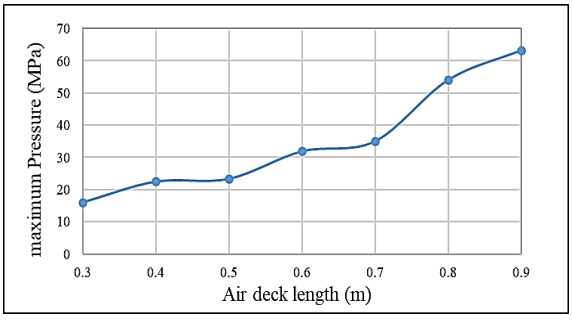

Figure 10. Maximum pressure applied to the highest element in the stemming.

Table 8. Maximum pressure changes ratio with rising air deck length on the highest element of stemming.

Charging pattern number	Air deck length (m)	Maximum pressure (MPa)	Changes ratio of Pressure	Average pressure changes
1	0.3	18.32	-	-
2	0.4	22.39	1.22	1.18
3	0.5	26.20	1.17	
4	0.6	31.81	1.21	
5	0.7	34.94	1.10	
6	0.8	54.00	1.55	1.58
7	0.9	86.70	1.61	

Table 9. Ratio of maximum velocity changes of throwing stemming with the increase air deck length.

Charging pattern number	Air deck length (m)	Velocity of throwing stemming (m/s)	Changes ratio of velocity	Average velocity changes
1	0.3	52.65	-	-
2	0.4	76.28	1.45	1.30
3	0.5	93.48	1.23	
4	0.6	108.94	1.17	
5	0.7	149.79	1.37	
6	0.8	398.98	2.66	2.39
7	0.9	843.88	2.12	

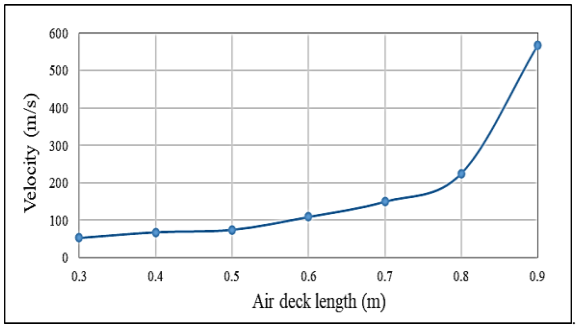

Figure 11. Maximum vertical velocity of the highest element at top of stemming.

comprehend the design principles of this method to increase productivity. To optimize the air deck blasting mechanism, the appropriate length of the air column should be used. In this study, the criterion for choosing the most optimal length of the air column is the damage zone achieved on the surface (or head of the hole).

According to the field test of Singh et al., single blast hole modelling was done and validated. In the performed modelling, the air deck length ratio was designed from 10.7% to 26.5%. After the finishing of the blasting processes, the amount of rock mass damage was measured in different charging patterns. The highest damage radius was observed for the air deck with a ratio of 21.9% (pattern no. 5). More damage indicates a more optimal use of the explosive energy due to the correct operation of the air deck blasting mechanism. In fact, the appropriateness of the length of the air column, stemming and the explosive has led to the largest damage zone for the air deck with a ratio of 21.9%, compared to the rest of the patterns.

In order to investigate the influencing factors on the damage radius of rock mass, the history of the maximum pressure applied to the highest point of the stemming column and the velocity of the stemming column movement were investigated. With increasing the length of the air deck, the pressure applied to the top of the stemming column increased. Also, for the air deck with a length greater than 0.7 meters (21.9%), as a result of shortening the stemming length, the energy of the explosive material is discharged quickly and the damage of the rock mass is reduced.

References

[1] Jimeno, CL., Jimeno, EL., & Carcedo, FJA. (1995). Drilling and Blasting of Rocks. Rotterdam, Netherlands: AA Balkema.

[2] Hustrulid, W. A. (1999). Blasting Principles for Open Pit Mining., Rotterdam, Netherlands: AA Balkema.

[3] Bakhshandeh Amnieh, H., & Bahadori, M. (2017). Numerical Analysis of the Primer Location Effect on Ground Vibration Caused by Blasting. International Journal of Mining and Geo-Engineering, 51(1), 53-62. dio: https://doi.org/10.22059/ijmge.2017.62153.

[4] Berta, G. (1990). Explosive - an Engineering tool, Italesplosivi, Milano.

[5] Saadatmand Hashemi, A., & Katsabanis, P. (2020). The effect of stress wave interaction and delay timing on blast-induced rock damage and fragmentation. Rock mechanics and rock engineering, 53, 2327-2346. Doi: https://doi.org/10.1007/s00603-019-02043-9.

[6] Melnikov, N. V., & Marchenko, L. N. (1970). Effective methods of application of explosive energy in mining and construction , 12th Symp on dynamic rock mechanics. AIME, New York, 350-378.

[7] Chiappetta, R. F., & Mammele, M. E. (1987). Analytical high-speed photography to evaluate air decks, stemming retention and gas confinement in presplitting, reclamation and gross motion applications. In Proceedings of the second international symposium on rock fragmentation by blasting. Society for Experimental Mechanics, Bethel, CT, USA, 257-301.

[8] Gao, F., Tang, L., Yang, C., Yang, P., Xiong, X., & Wang, W. (2023). Blasting-induced rock damage control in a soft broken roadway excavation using an air deck at the blasthole bottom. Bulletin of Engineering Geology and the Environment, 82(3). 97. doi: https://doi.org/10.1007/s10064-023-03087-6.

[9] Zhang, Z. X. (2016). Rock fracture and blasting: theory and applications. Butterworth-Heinemann.

[10] Zhang, Z. X. (2011). Reducing eyebrow break caused by rock blasting in Malmberget mine. Fragblast, 1–10.

[11] Sazid, M., & Singh, T. N. (2013). Mechanism of Air Deck technique in rock blasting –A BRIEF REVIEW. In 4th Indian Rock Conference, 29-41.

[12] Chiappetta, F. (2004). New blasting technique to eliminate subgrade drilling, improve fragmentation, reduce explosive consumption and lower ground vibration. Journal of explosive engineering, 21(1), 2-10.

[13] Rommayawes, S., Leelasukseree, C., & Jaroonpattanapong, P. (2014). Influence of Air Deck length on fragmentation in Quarry blasting. European Scientific Journal, edition vol.3 ISSN: 1857 – 788.

[14] Arefmand, E., Bakhshandeh Amnieh, H., Majdi, A. & Vahidi, M. (2024). Numerical Analysis of Borehole Pressure History and Rock Mass Damage Induced by Conventional and Air Deck Explosion Methods. Journal of Mineral Resources Engineering, 9(4), 81-93. https://doi:10.30479/jmre.2024.19413.1668.

[15] Mel'Nikov, N. V., Marchenko, L. N., Zharikov, I. F., & Seinov, N. P. (1979). A method of enhanced rock breaking by blasting. Soviet Mining, 15(6), 565-572.

[16] Fourney, W.L, Barker, D.B., & Holloway, DC. (1981). Model studies of explosive well simulation techniques. Int J Rock Mechs Min Sci Geomech Abs, 18,113–127.

[17] Liu, L., & Katsabanis, P.D. (1996). Numerical modeling of the effects of air decking/decoupling in production and controlled blasting. In Proceeding 5th international conference on rock fragmentation by blasting. A. A. Balkema, Rotterdam. 319–330.

[18] Lu, W., and Hustrulid, W. (2003). A further study on the mechanism of air-decking. Fragblast 7(4), 231–255. dio: http://dx.doi.org/10.1076/frag.7.4.231.23532.

[19] Lou, X., Wang, Z., Chen, B., & Yu, J. (2018). Theoretical calculation and experimental analysis on initial shock pressure of borehole wall under axial decoupled charge. Shock and Vibration. https://doi.org/10.1155/2018/7036726.

[20] Mead, D.J., Moxon, N.T., Danell, R.E., & Richardson, S.B. (1993). The use of air-decks in production blasting. In: Proceedings of the 19th annual conference on explosives and blasting technique, international society of explosives engineers, Cleveland, Ohio, USA, 437–443.

[21] Saharan, M. R., Sazid, M., & Singh, T. N. (2017). Explosive energy utilization enhancement with air-decking and stemming plug,'SPARSH'. Procedia engineering, 191, 1211-1217. dio:http://creativecommons.org/licenses/by-nc-nd/4.0/.

[22] Chen, ZB., Cheng, LY., Zhong, MS., Xu, QJ., Wen, ZL. & Sun, F. (2017). Bottom inert medium in deck charging blasting experiment. Eng Blasting, 23(1):12–15. https://doi.org/10.3969/j.issn.1006-7051.2017.01.003

[23] Balakrishnan, V., and Pradhan, M. (2018). Explosive consumption reduction by introducing hollow plastic tubes in explosive column. APRN Journal of Engineering and Applied Sciences. 13(14), 4325-4330.

[24] Jang, H., Handel, D., Ko, Y., Yang, H. S., & Miedecke, J. (2018). Effects of water deck on rock blasting performance. International Journal of Rock Mechanics and Mining Sciences, 112, PP. 77-83. https://doi.org/10.1016/j.ijrmms.2018.09.006.

[25] Bakhshandeh Amnieh, H., Arefmand, E., and Porghasemi Saghand, M. (2019). Controlling Backbreak and Improving Technical and Economic Parameters in Mishdovan Iron Ore Mine. Mineral Resources engineering. https://doi.org/10.30479/jmre.2019.10436.1251.

[26] Bakhshandeh Amnieh, H., Arefmand , E., and Porghasemi Saghand, M. (2020). A study of rock fragmentation caused by Power Deck and conventional blasting in Mishdovan iron ore mine. 7th Iranian Rock Mechanics Conference (IRMC7),Tehran, Iran.

[27] Cheng, R., Zhou, Z., Chen, W., & Hao, H. (2022). Effects of axial air deck on blast-induced ground vibration. Rock Mechanics and Rock Engineering,1-17. doi: https://doi.org/10.1007/s00603-021-02676-9.

[28] Zhang, GJ. (1996). A study of free toe-space explosive loading and its application in open pit blasts. In: Proceedings of 5th international symposium on rock fragmentation by blasting, 313–318.

[29] Jhanwar, J.C., & Jethwa, J.L. (2000). The use of air-decks in production blasting in an open pit coal mine. Geotech Geol Eng 18:269–287. Doi: https://doi.org/10.1023/A:1016634231801.

[30] Jhanwar, J.C., Jethwa, J.L., & Reddy, A.H. (2000). Influence of air-deck blasting on fragmentation in jointed rocks in an open pit manganese mine. Eng Geol 57:13–29. doi: https://doi.org/10.1016/S0013-7952(99)00125-8.

[31] Jhanwar, J. C. (2011). Theory and practice of air-deck blasting in mines and surface excavations: a review. Geotechnical and Geological Engineering, 29(5), 651-663. Doi: https://doi.org/10.1007/s10706-011-9425-x.

[32] Saqib, S., Tariq S. M., & Ali, z. (2015). Improving rock fragmentation using airdeck blasting Technique, Pak. J. Engg. & Appl. Sci, Vol. 17, 46-52.

[33] Singh, T. N., Sazid, M., & Saharan, M. R. (2012). A study to simulate air deck crater blast formation-a numerical approach. In ISRM International Symposium-Asian Rock Mechanics Symposium (pp. ISRM-ARMS7). ISRM.

[34] Qiu, X., Hao, Y., Shi, X., Hao, H., Zhang, S., & Gou, Y. (2018). Numerical simulation of stress wave interaction in short-delay blasting with a single free surface. PLOS one, 13(9), e0204166. doi: https://doi.org/10.1371/journal.pone.0204166.